

Supporting Information

Temperature Dependence of the Air/Water Interface Revealed by Polarization Sensitive Sum-Frequency Generation Spectroscopy

Daniel R. Moberg, Shelby C. Straight, and Francesco Paesani*

*Department of Chemistry and Biochemistry, University of California, San Diego, La Jolla,
California 92093, United States*

E-mail: fpaesani@ucsd.edu

Structure of Water Slabs

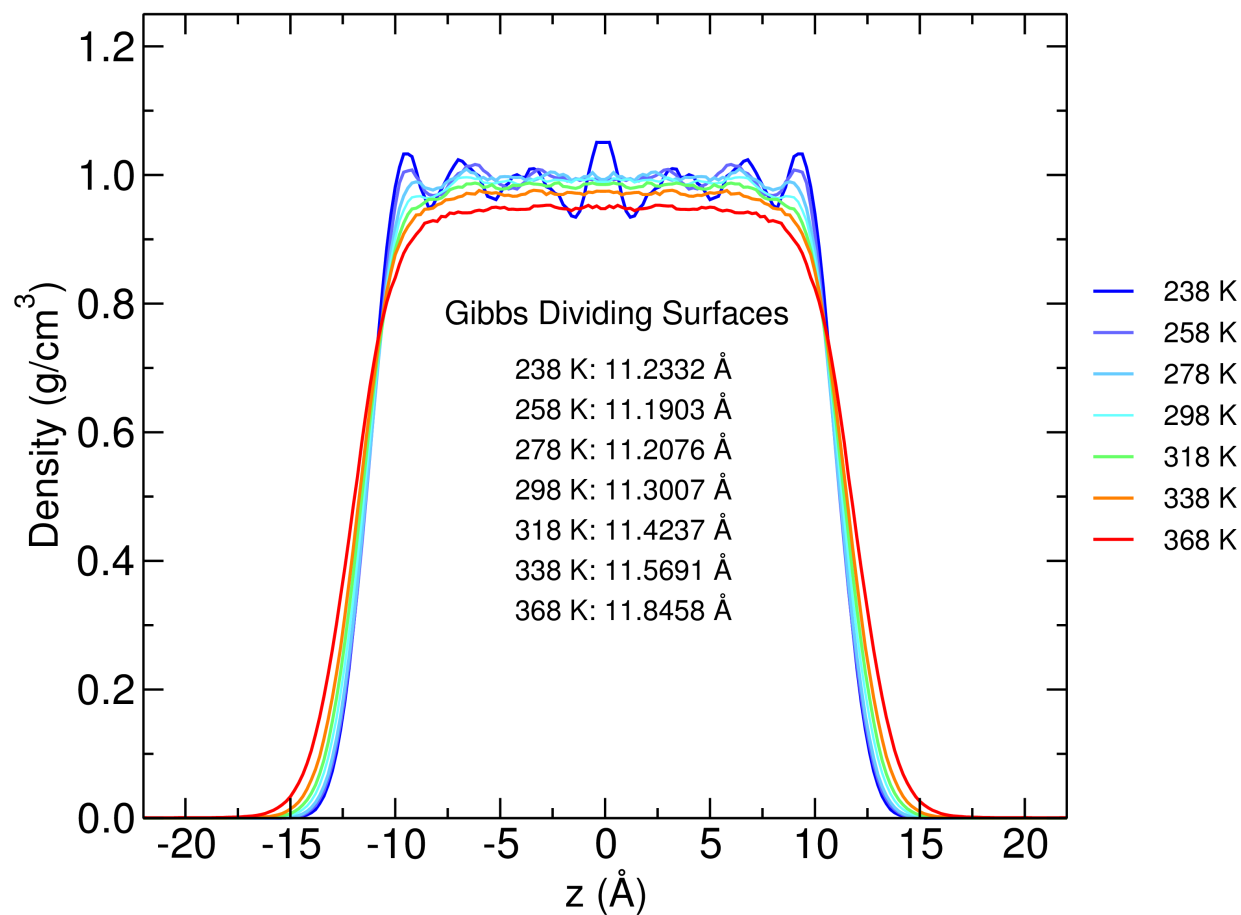


Figure S1: Density profiles of water slabs as a function of temperature. The Gibbs dividing surfaces for each temperature are also included.

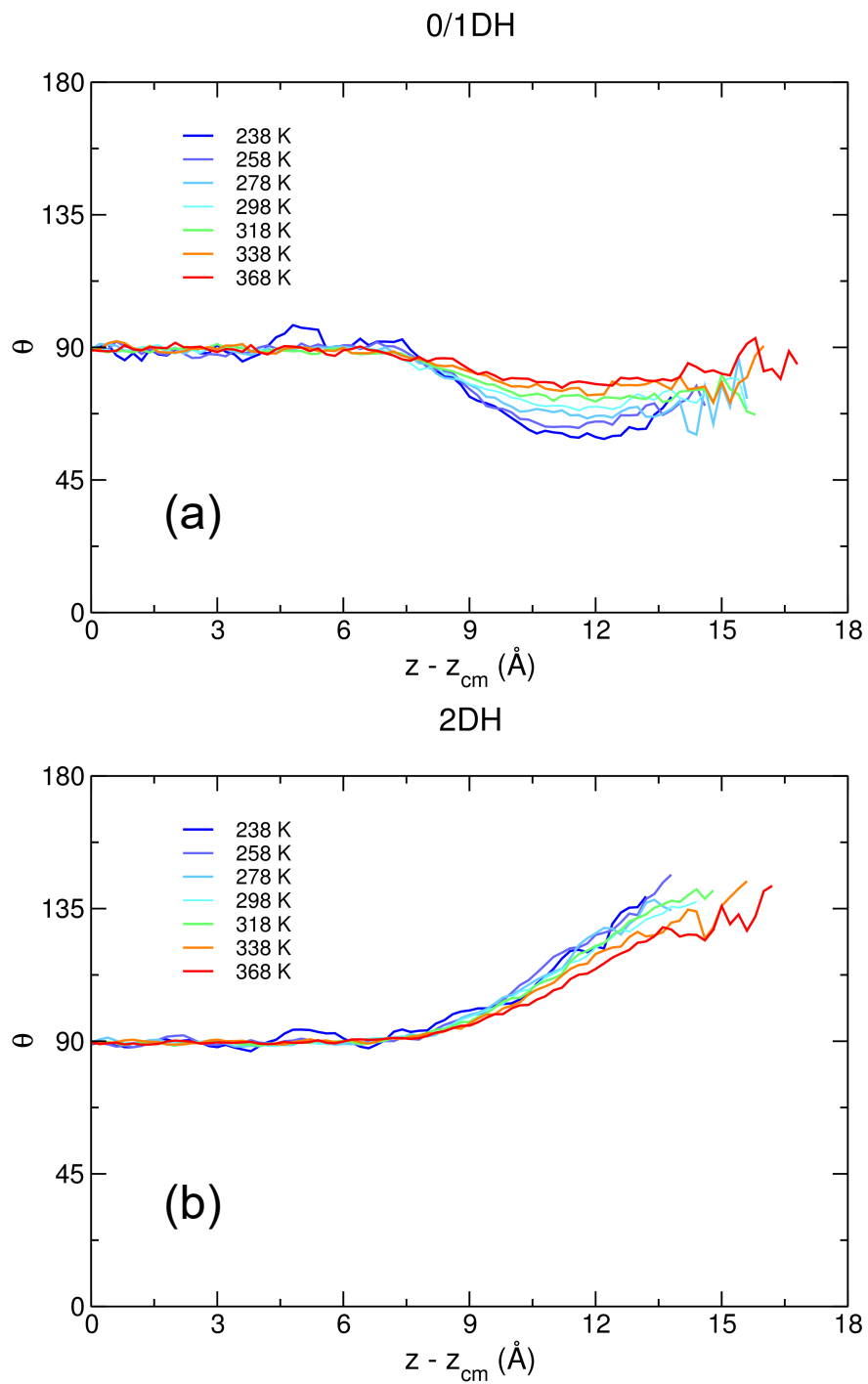


Figure S2: Temperature dependence of the average angle for water molecules as a function of distance from the center of mass of simulation slab for (a) 0/1DH and (b) 2DH.

$\chi_{ijk}^{(2)}$ Spectra - No Fresnel Factors

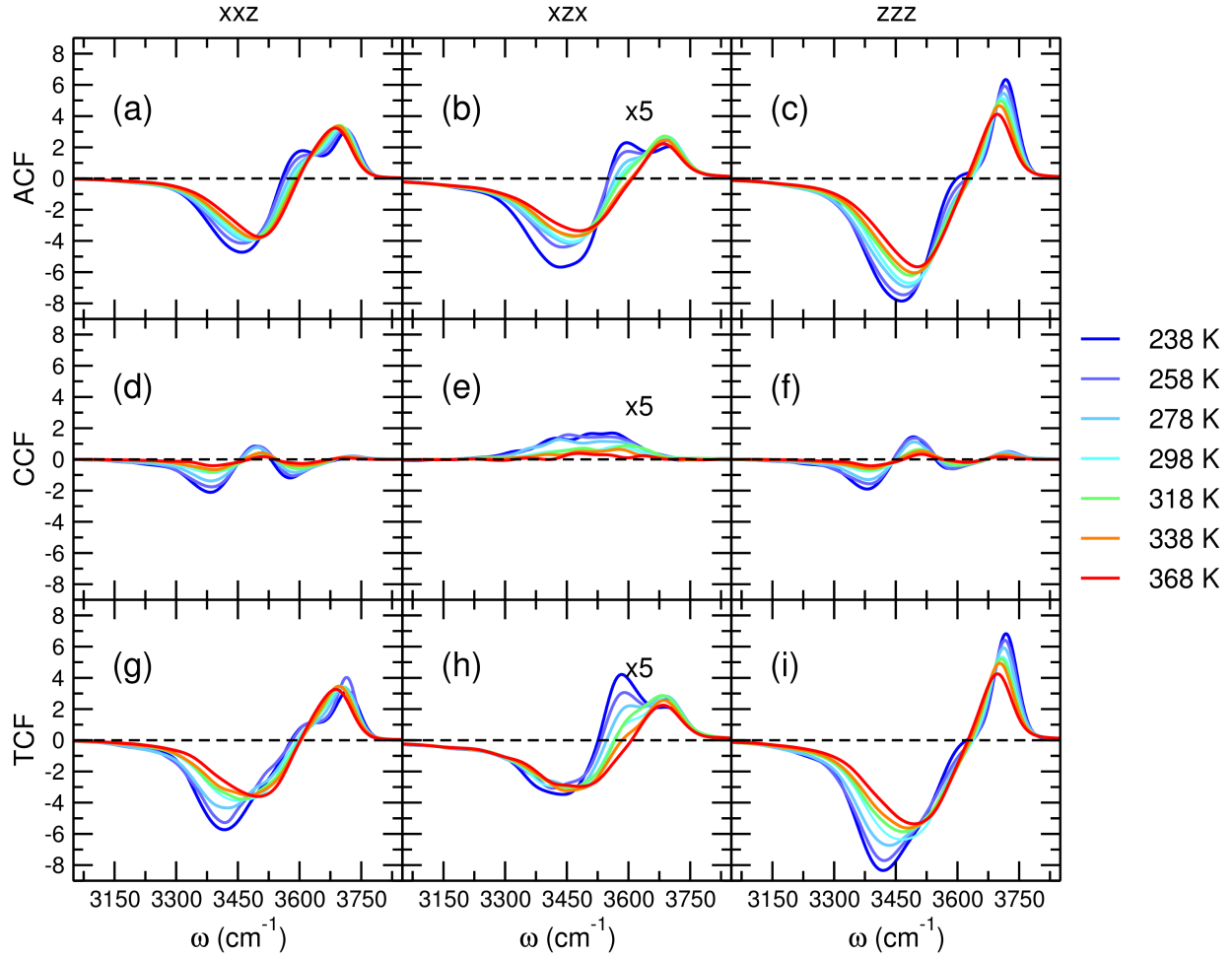


Figure S3: Polarization and temperature dependent vSFG spectra of the OH stretching region at the air/water interface. From top-to-bottom: auto-correlation contribution (ACF, a-c), cross-correlation contribution only (CCF, d-f), and total contribution (TCF, g-i) to the vSFG spectra with intermolecular cut-off of 4.0 Å. From left to right: imaginary components of $\chi_{xxz}^{(2)}(\omega)$, $\chi_{xzx}^{(2)}(\omega)$, and $\chi_{zzz}^{(2)}(\omega)$. All $\chi_{pqr}^{(2)}(\omega)$ were calculated according to Eq. 2 in the main text and normalized relative to $k_B T_{298}$ (see Table S1).

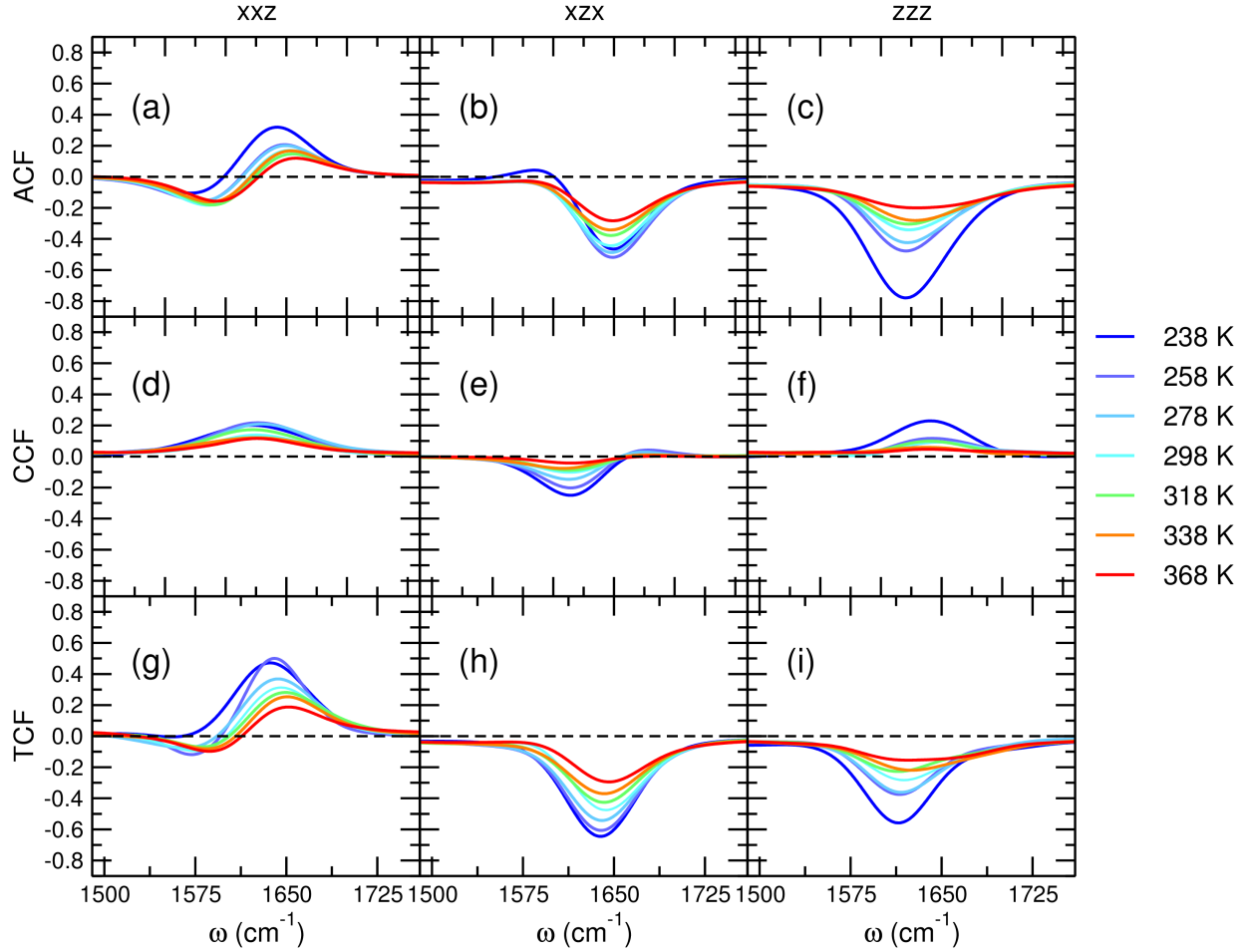


Figure S4: Polarization and temperature dependent vSFG spectra of the OH bending region at the air/water interface. From top-to-bottom: auto-correlation contribution (ACF, a-c), cross-correlation contribution only (CCF, d-f), and total contribution (TCF, g-i), to the vSFG spectra with intermolecular cut-off of 4.0 Å. From left to right: imaginary components of $\chi_{xxz}^{(2)}(\omega)$, $\chi_{xzx}^{(2)}(\omega)$, and $\chi_{zzz}^{(2)}(\omega)$. All $\chi_{pqr}^{(2)}(\omega)$ were calculated according to Eq. 2 in the main text and normalized relative to $k_B T_{298}$ (see Table S1).

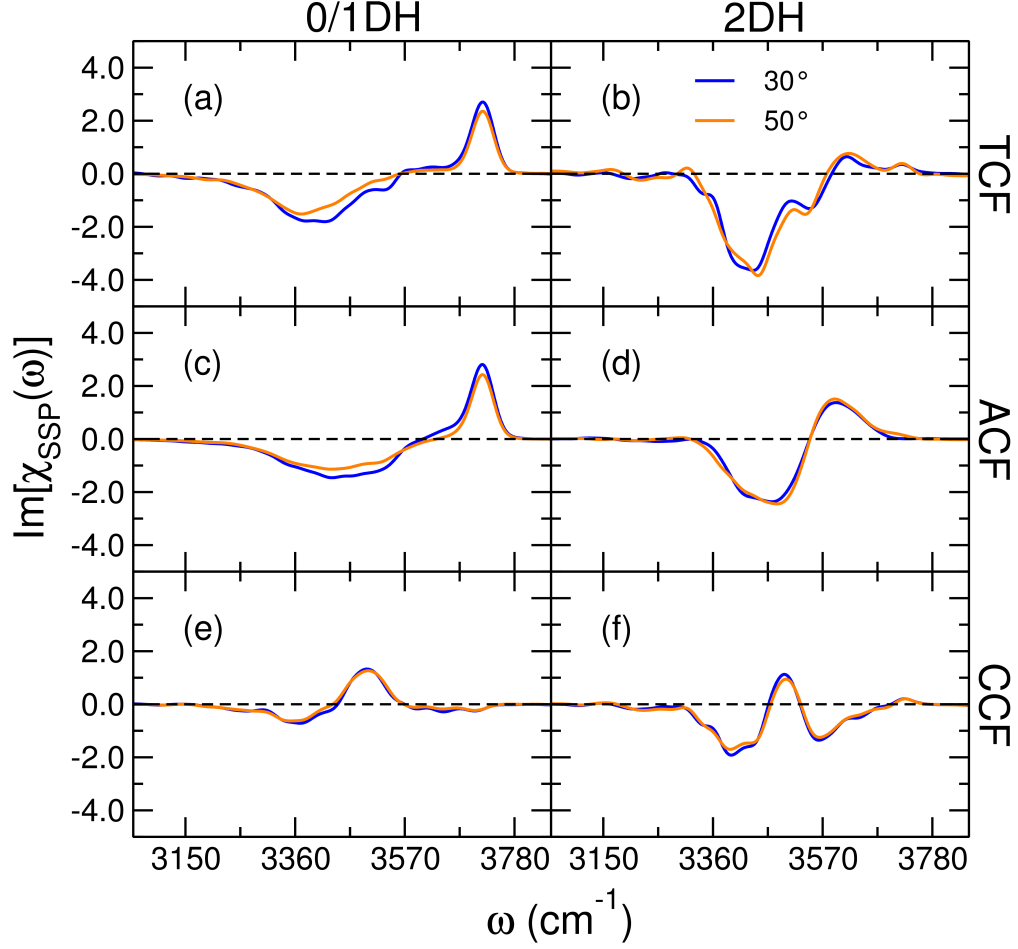


Figure S5: Comparison of (a, c, e) 0/1DH and (b, d, f) 2DH spectra using hydrogen bond angle cutoffs of 30° and 50° at 238 K. The top row contains the total correlation functions, the second row contains the autocorrelation function, and the third row contains cross-correlation function contributions. All $\chi_{pqr}^{(2)}(\omega)$ were calculated according to Eq. 2 in the main text and normalized relative to $k_B T_{298}$ (see Table S1).

Table S1: Redshift applied to each spectrum in the stretching region based on a linear fit to difference between classical and centroid molecular dynamics simulations performed in Ref. 1.

| Temperature (K) | Stretching redshift (cm ⁻¹) | Bending redshift (cm ⁻¹) |
|-----------------|---|--------------------------------------|
| 238 | 155.96 | 59.39 |
| 258 | 157.62 | 57.97 |
| 278 | 159.27 | 56.56 |
| 298 | 160.93 | 55.14 |
| 318 | 162.59 | 53.73 |
| 338 | 164.24 | 52.31 |
| 368 | 166.73 | 50.19 |

References

- (1) Reddy, S. K.; Moberg, D. R.; Straight, S. C.; Paesani, F. Temperature-Dependent Vibrational Spectra and Structure of Liquid Water from Classical and Quantum Simulations with the MB-pol Potential Energy Function. *J. Chem. Phys.* **2017**, *147*, 244504.